Kovove Mater. 57 2019 1–9
DOI: 10.4149/km_2019_1_1

Microstructure and thermal stability of the Cu-ZrB_2 and CuCr1Zr-ZrB_2 composites prepared by gas pressure infiltration

A. Opálek[1]*, N. Beronská[1], Š. Nagy[1], T. Dvorák[1], P. Štefánik[1], T. Švantner[1], P. Švec[2], K. Iždinský[1]

[1]*Institute of Materials and Machine Mechanics, Slovak Academy of Sciences, Dúbravská cesta 9, 845 13 Bratislava, Slovak Republic*
[2]*Institute of Physics, Slovak Academy of Sciences, Dúbravská cesta 9, 845 11 Bratislava, Slovak Republic*

Received 9 September 2018, received in revised form 5 November 2018, accepted 15 November 2018

Abstract

Composite materials based on Cu matrix have a wide range of applications because of their extraordinary features such as high thermal conductivity and high mechanical strength. The preparation of Cu-ZrB_2 and CuCr1Zr-ZrB_2 composites via gas pressure infiltration technology is described in this work. In contrast to most ceramic materials, ZrB_2 is electrically and thermally conductive. All tested samples, i.e. prepared from the ZrB_2 porous preform with a porosity of 40 % were infiltrated with molten Cu or CuCr1Zr alloy. Microstructure and homogeneity after infiltration were examined by SEM-EDS microscopy. The interface between the Cu matrix and ZrB_2 ceramics was explored by TEM microscopy. As-infiltrated composites were thermally cycled up to 800 °C with heating and cooling rates of 3 °C min^{-1} in an argon atmosphere.

K e y w o r d s: Cu-ZrB_2 composite materials, metal matrix, gas pressure infiltration, thermal treatment

1. Introduction

Even though many high-temperature construction materials are used in more practice application, there is a constant demand for new ones. At present, the development of new materials is related to the knowledge and studies of composite materials, where new advantageous properties can be achieved due to the contributions of particular components. In many papers, special interest is focused on metal-ceramic composites with porous reinforcing networks, which are different from the traditional composites usually composed of discrete fibres, whiskers or particles dispersed within a matrix phase [1].

The metal-ceramic composite formed by ultra-high temperature ceramics sintered to skeleton preform via powder metallurgy and subsequently infiltrated with metal phase could be attractive for plasma spark-resistive electrode material used in many plasma technologies, e.g. plasma cutting, welding, sintering, etc. [2]. Many metal-ceramic composites prepared via different technologies have been reported worldwide. However, these studies were usually focused on mechanical properties important in engineering application, not in high-temperature applications which are related to the ablation performance and thermal properties characterization such as high thermal conductivity and low thermal expansion. Copper (Cu) with its high thermal conductivity (401 $W\,m^{-1}\,K^{-1}$), good electrical conductivity and availability is one of the best-known metals used for applications in electronics and electrical engineering. On the other hand, copper is limited by its melting point (1083 °C) and higher thermal expansion ($16 \times 10^{-6}\,K^{-1}$). From [1] traditional copper infiltrated tungsten composite (Cu/W) with special spatial inter-connected structure is known. Cu/W composite has high strength, high thermal shock resistance and high ablation resistance at elevated temperatures. The main disadvantage of Cu/W composite is that it has a high density of up to 16 $g\,cm^{-3}$. Another type of composites used for higher temperature applications known from [3, 4] are

*Corresponding author: tel.: +421232401051; e-mail address: andrej.opalek@savba.sk

composites combined with ultra-high temperature ceramics (UHTCs), resp. in combination with transition metal diborides of group IV (e.g. zirconium diboride ZrB_2). The combination of SiC and ZrB_2 exhibits high electrical conductivity, superior oxidation resistance, high mechanical strength which can be used as a conductive material or electrode at high temperature [3]. However, in connection with Si, the thermal conductivity of SiC-ZrB_2 could be lower than usually expected in high-temperature applications.

Chamberlain et al. [5] introduced zirconium diboride (ZrB_2) as a transition metal boride that crystallizes into a hexagonal crystal structure of the AlB2 type. It consists of alternating layers of hexagonally closed packed metal atoms (M) and graphite-like boron (B) stacked in an MBMBMB sequence. Strong covalent bonding is formed between boron-boron and metal-boron atoms, while the close-packed metal layers exhibit characteristics consistent with metallic bonding. The combination of covalent and metallic bonding gives ZrB_2 an unusual combination of properties.

ZrB_2 has a high melting point of 3250 ℃ what makes it an attractive heat-resistant material. Combination of high melting point and other specific properties as e.g. high strength (~ 500 MPa), high hardness (23 GPa), low electrical resistivity ($10^{-5}\,\Omega$ cm), chemical inertness, make ZrB_2 attractive as an ultrahigh-temperature ceramic used for high thermal structural applications, e.g. refractory linings, high temperature electrodes, cutting tools, protection systems on hypersonic flight vehicles. Various studies on the thermochemical and thermophysical properties have been performed for ZrB_2 ceramics, revealing that e.g. significant differences in thermal conductivity (from 24 to 60 $W\,m^{-1}\,K^{-1}$) could be due to impurities or the different porosity of studied samples [2, 5–8].

Copper-based zirconium composite (Cu/ZrB_2) seems to be an excellent spark-resistive electrode material. The employment of Cu/ZrB_2 composite as an electrode in plasma applications was described in detail in [2] by Norasetthekul et al. The addition of Cu appears quite necessary considering the poor thermal conductivity of ceramic and low thermal stress. As plasma strikes the electrode surface, Cu melts and/or vaporizes before ZrB_2. It is possible because of high thermal conductivity and a low melting point of Cu. Thus, excess heat is carried away from the surface by the Cu until the thermal stress on the ceramic decreases, when the spark is extinguished or when the arc/spark moves to another surface location. Although the metal melts and vaporizes initially, it tends to resolidify quickly back to surface after spark has disappeared [2].

However, the combination of ZrB_2 ceramics with Cu matrix faces several difficulties. Much depends on the technology of the composite preparation. Manufacturing of products based on the ZrB_2 ceramics is difficult because treatment of ZrB_2 is almost impossible due to its high hardness [9]. Therefore, a simpler way for composite preparation could be the gas pressure infiltration technology followed by machining of the sample to the desired shape. However, this also includes some difficulties. One of them is no wetting [10], and another one is the lack of chemical activity in the Cu/ZrB_2 binary system resulting in poor bonding at the interface, with implications towards the thermal stability at high temperatures. Therefore, suitable active elements can be added to the copper matrix to improve the interface.

Muolo et al. [10, 11] have described the wettability of ZrB_2 with molten Cu and Ag, which belong to best metal conductors. However, neither Cu nor Ag wet the ultra-high temperature ZrB_2 ceramics. A sharp decrease in contact angle was obtained when AgCuZr alloy was used. In comparison with AgZr alloy, the same result was measured. Primarily, using Ag metal as a matrix would be uneconomical. From the same literature, the purpose to improve the wettability of Cu with the addition of Ni powder to ZrB_2 ceramics was successful. When Ni (4 wt.%) as a sintering add was used Cu wetted the ceramic substrate [10, 11]. The main disadvantage of Ni as an additive could be the potential decrease of thermophysical properties of the composite at higher temperatures [5]. Successful manufacturing of Cu/ZrB_2 composites via gas pressure infiltration, the study of their structure and thermal stability are the main objectives of this paper.

Table 1. The chemical composition of applied Cu and CuCr1Zr alloy as-obtained by light optical spectroscopy (wt.%)

CuCrZr alloy	Cu	Cr	Zr	Fe	Si	Zn	Ni
	98.9	0.756	0.134	0.049	0.022	0.015	0.01
Cu	Cu	Zn	Fe				
	99.9	0.014	0.015				

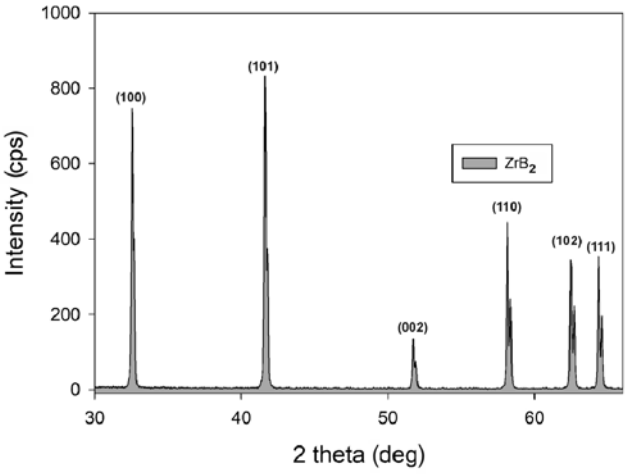

Fig. 1. XRD analysis of the structure of ZrB_2 bulk compact.

2. Materials and methods

Composite samples were manufactured using ultra-high temperature ZrB_2 ceramic sintered bulk (99.5 % purity, density of 60 %) delivered by China Rare Metal Material Co., Ltd., and pure Cu, resp. CuCr1Zr alloy from Deutsches Kupferinstitute. The nominal chemical composition of the CuCr1Zr alloy was as follows: Cu (rest), Cr (0.5–1.2 %), Zr (0.03–0.3 %), Fe (0.08 %), Si (0.1 %). Cu/ZrB_2 composites were prepared by gas pressure infiltration technology.

ZrB_2 bulk preform was fixed in the molybdenum cage with the dimensions $10 \times 20 \times 40\,mm^3$. Fixed preform had been inserted into a high-pressure autoclave and preheated in a vacuum of $\sim$ 60 Pa. In these experiments, the graphite crucibles were used. Once the infiltration temperature of 1185 ℃ had been reached, the prepared preform was immersed into a molten metal matrix. Nitrogen gas pressure was applied up to 5 MPa within 120 s. As-infiltrated samples were pulled out from the molten matrix and cooled down in autoclave outside the heated zone. Two types of composites, i.e. ZrB_2 preform infiltrated with Cu, and CuCr1Zr alloy respectively were prepared and tested. Structural and morphological observations on as-received samples were performed with

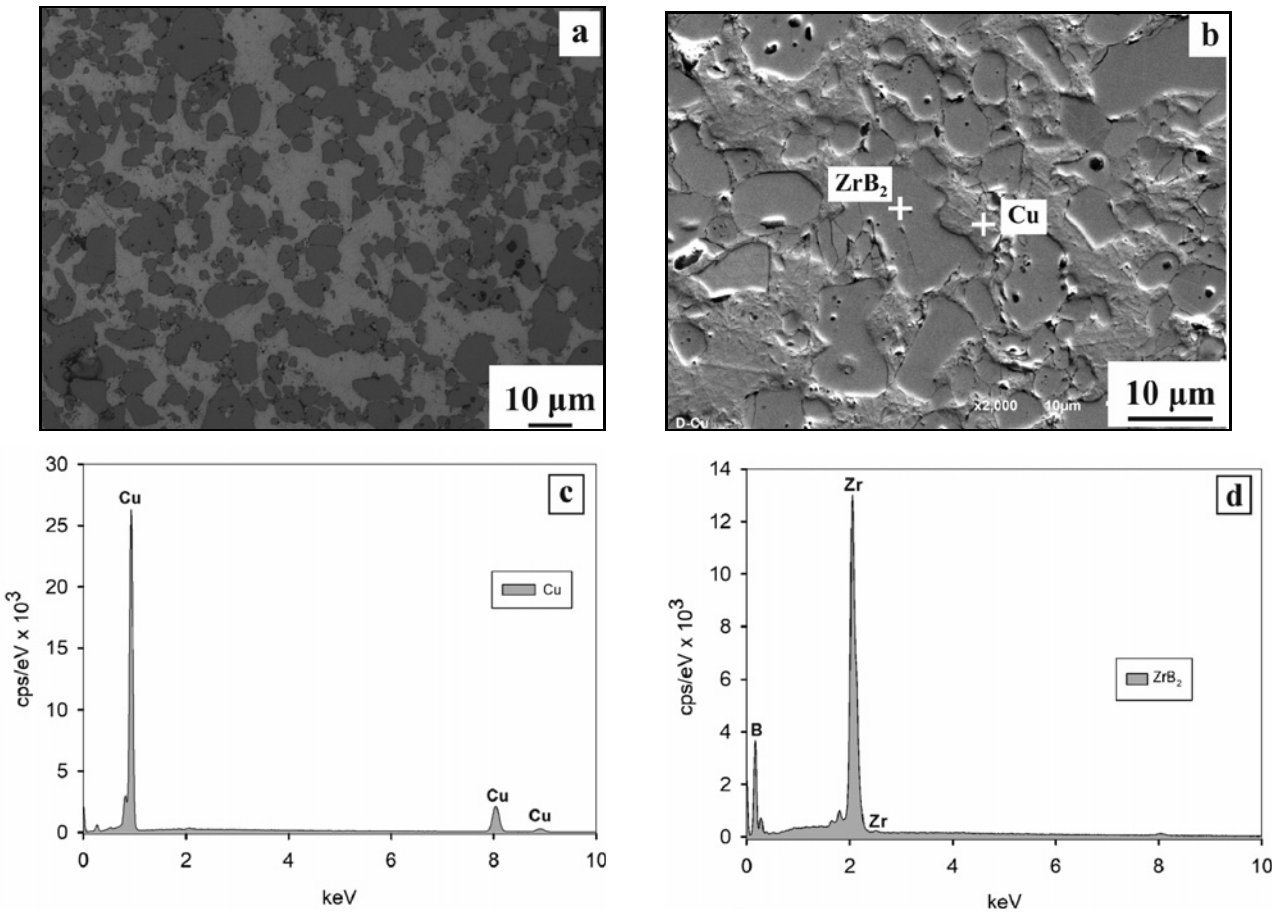

Fig. 2. The microstructure of Cu/ZrB_2 composite determined by LM (a) and SEM (b). EDX spectra obtained by point analysis in Cu (c), and ZrB_2 (d).

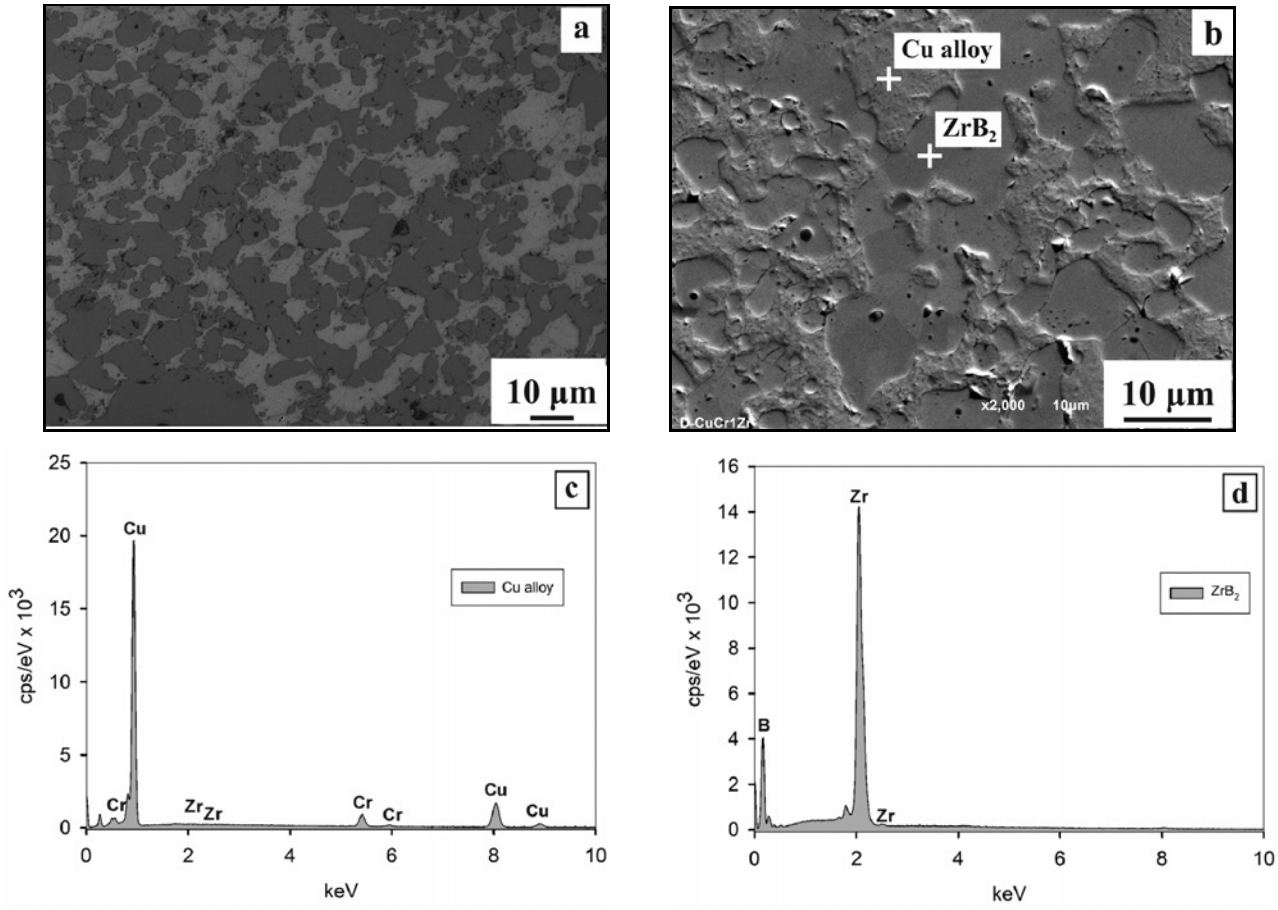

Fig. 3. The microstructure of CuCr1Zr/ZrB_2 composite determined by LM (a) and SEM, (b) EDX spectra obtained by point analysis in Cu alloy (c), and ZrB_2 (d).

light microscopy (LM – OLYMPUS GX51) and secondary electron microscopy (SEM – JEOL JSM 6610). Phase structures and chemical composition were analysed using X-ray diffraction (Bruker AXS D4 Endeavor diffractometer with Bragg-Brentano geometry and Cu Kα radiation), light emission spectrometry (SPECTROMAX x LMX06) as well as energy dispersive X-ray spectroscopy (EDS-X-Maxx Oxford Instruments). Transmission electron microscopy (TEM) observations using a JEOL TEM 1200EX microscope operated at 100 kV were performed to reveal the composite interfaces. Thin foils for TEM studies were prepared using mechanical grinding followed by ion milling with a GATAN PIPS II machine. The thermal expansion measurements were used to test the thermal stability of composites. Samples with the dimensions of $4 \times 4 \times 10\,mm^3$ were subjected to 5 consecutive heating and cooling cycles at the heating/cooling rate of $3\,℃\,min^{-1}$ in an argon atmosphere using NETZSCH DIL 402 Expedis Select dilatometer equipped with an alumina holder. Samples were cycled in the temperature range from 30 to 800 ℃. Instantaneous CTE values were calculated from the strain-temperature curves.

3. Results

3.1. Chemical and structural analysis

The chemical composition of applied Cu and CuCr1Zr alloy as-obtained by light optical spectroscopy is presented in Table 1. It is within limits declared by the supplier.

X-ray diffraction spectrometry revealed the purity and the crystal structure of the ZrB_2 preform used in experiments. The measurement of the ZrB_2 preform skeleton confirmed pure hexagonal crystal structure according to PDF 00-034-0423 as presented in Fig. 1.

3.2. Structural studies

The microstructure of Cu/ZrB_2 composite as-revealed by LM is presented in Fig. 2a. The copper is in light grey colour, and ZrB_2 ceramics is in dark grey. The similar microstructure was observed at the top and bottom of the infiltrated samples. This proved that copper was sufficiently infiltrated into the whole volume of the sample. Therefore, it is evident that Cu/ZrB_2 composites were homogeneous throughout

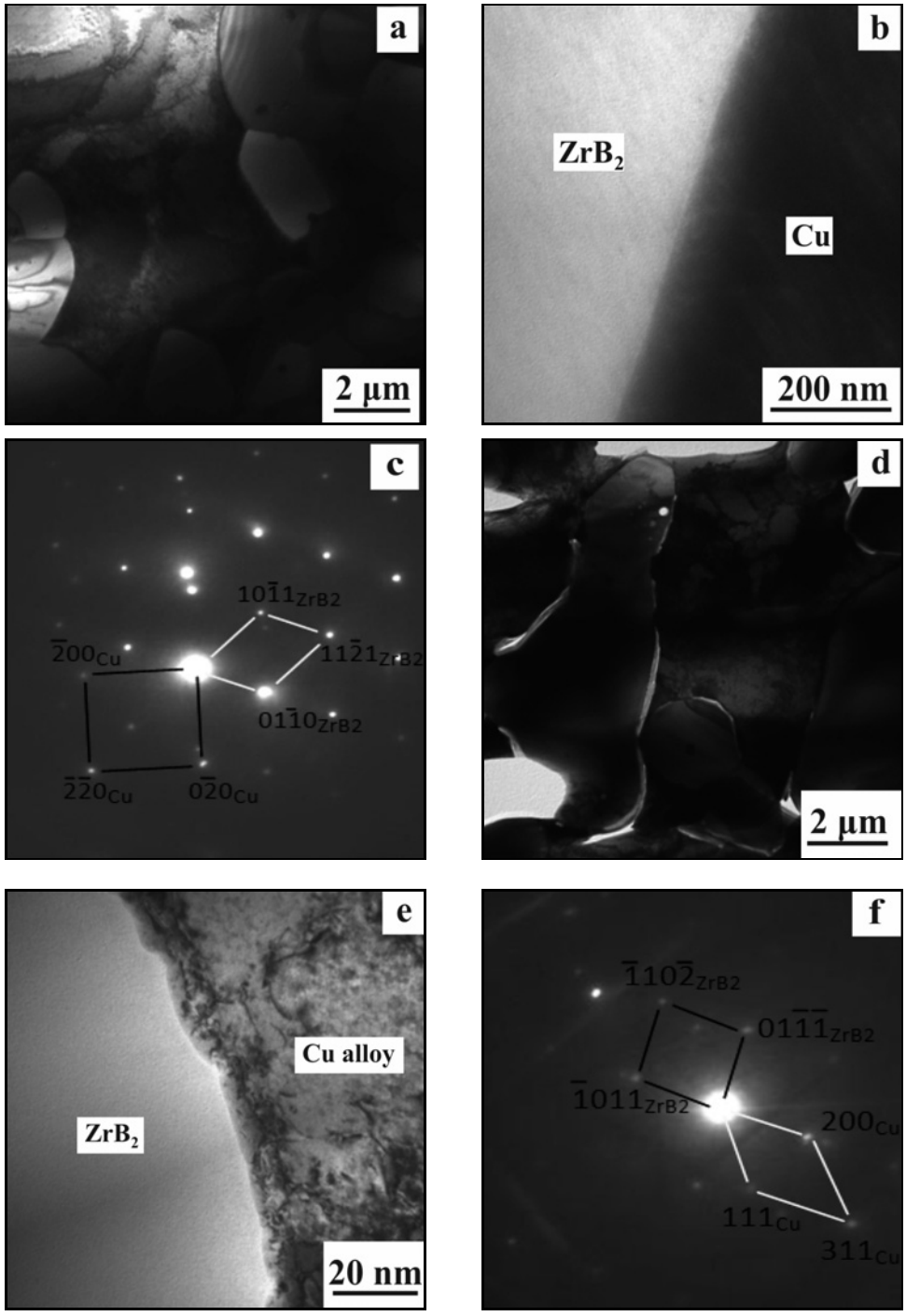

Fig. 4. TEM micrographs of ZrB2 preform/Cu microstructure (a), ZrB2 preform/Cu interface (b), SAED of interface area (c), ZrB_2/CuCrZr microstructure (d), ZrB_2/CuCrZr interface (e), and SAED of interface area (f).

the whole sample. Although some pores were rarely observed, neither zones without Cu, nor cracks, cavities and other defects with negative effect on the microstructure and thus the thermal properties were observed. The composite structure as revealed by SEM is presented in Fig. 2b confirming the results obtained by LM observations. The EDX spectra corresponding to Cu and ZrB_2 are presented in Figs. 2c,d.

The microstructure of CuCr1Zr/ZrB_2 composite as-revealed by LM is presented in Fig. 3a. The composite was quite homogeneously infiltrated as well. The pores are again located mostly inside the ZrB_2 preform. They can be regarded as closed pores that could not have been filled with penetrating molten matrix during infiltration. The composite structure as revealed by SEM is presented in Fig. 3b confirming

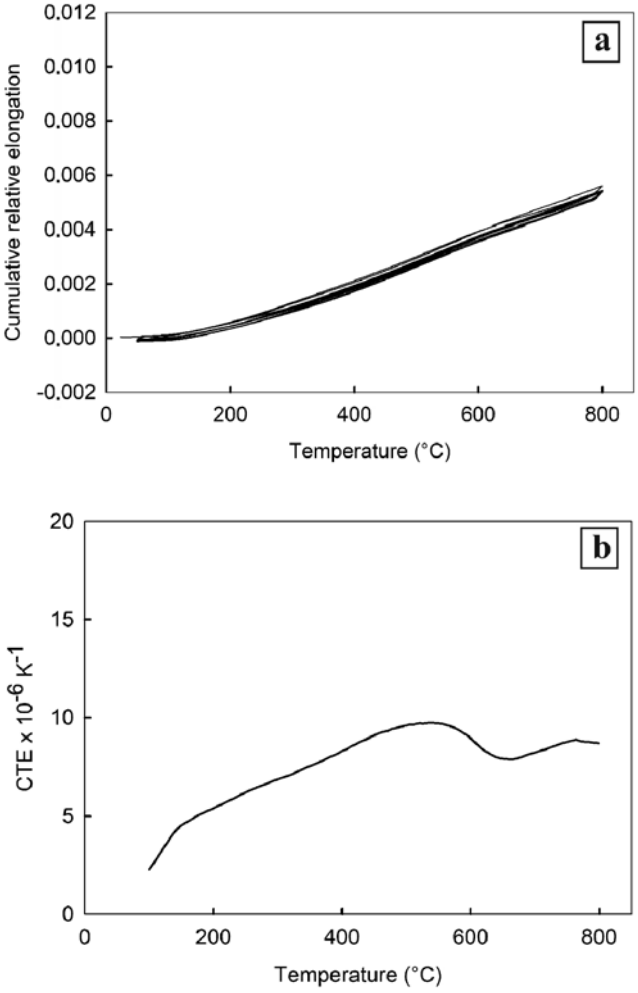

Fig. 5. Cumulative relative elongation of ZrB_2 preform subjected to 5 heating/cooling cycles to the temperature of 800 °C (a) with corresponding coefficients of thermal expansion (b).

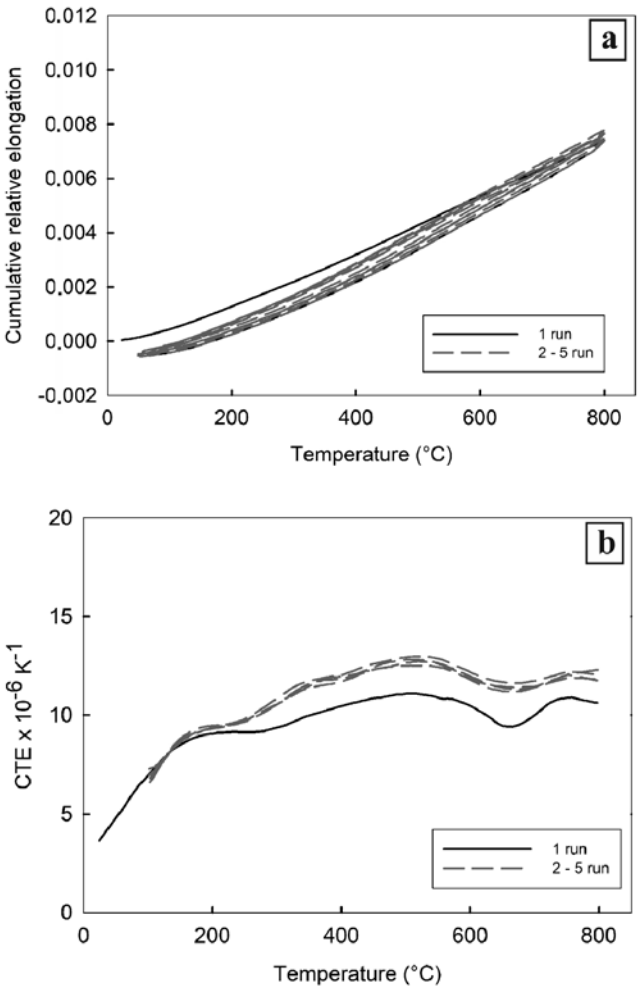

Fig. 6. Cumulative relative elongation (a) and coefficient of thermal expansion (b) of the ZrB_2 porous preform infiltrated with pure Cu.

the results obtained by LM observations. The corresponding EDX spectra corresponding to CuCr1Zr and ZrB_2 are presented in Figs. 3c,d.

The interfaces of both types of composites were further analysed by TEM. Relevant microstructures, interfaces and corresponding SAED patterns are presented in Fig. 4. The ceramic phase (Figs. 4a,d) appears as interconnected spherical objects surrounded by the matrix phase. The interfaces with good detectable borders are presented in higher magnifications in Figs. 4b,e. Small amounts of micropores on interfaces were also observed. The diffraction patterns in Figs. 4c,f taken from the interface areas correspond to hexagonal ZrB_2 phase and cubic Cu. For composite Cu/ZrB_2, the orientation relationship is $[004_{Cu}//[01-1]_{ZrB_2}$, and for composite $CuZrCr/ZrB_2$ is $[10-1]_{Cu}//[1-11]_{ZrB_2}$. No other phases were identified on the interface.

3.3. Thermal expansion

Thermal expansion measurements are sensitive to any phase changes in the tested material, and repeated heating/cooling cycles indicate the structural stability of the composite subjected to thermal stresses resulting from different coefficients of thermal expansion. The thermal expansion curves with corresponding coefficients of thermal expansion for ZrB_2 as-received bulk perform are presented in Fig. 5.

The thermal expansion curves with nearly coincident courses indicate the stability of the preform subjected to 5 consecutive heating/cooling cycles in the range of tested temperatures. The temperature dependence of CTE indicates particular deflection from the linear growth to a linear decrease in the temperature range 510 to 630 °C.

The thermal expansion curves with corresponding coefficients of thermal expansion for the Cu/ZrB_2 composite are presented in Fig. 6. The thermal expan-

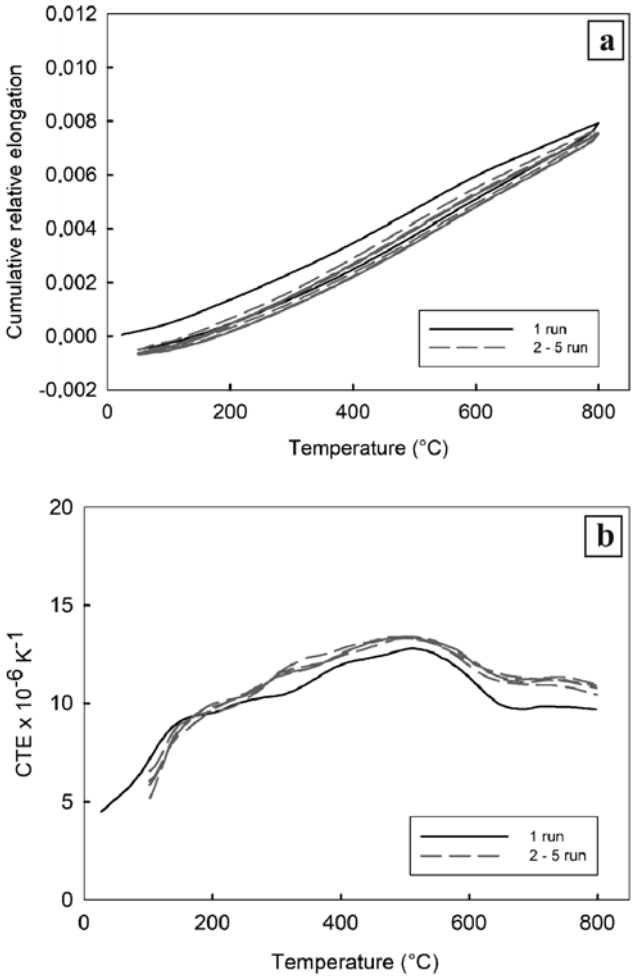

Fig. 7. Cumulative relative elongation (a) and coefficient of thermal expansion (b) of the ZrB_2 porous preform infiltrated with CuCr1Zr alloy.

sion in the first cycle is slightly different when compared to 2–5 cycles. This is due to the release of manufacturing thermal stresses built during the cooling from the infiltration temperature 1185 ℃. The CTE of the composite is slightly higher when compared with pure ZrB_2 bulk preform. However, the deflection in CTE curve is similar indicating that the ZrB_2 bulk preform qualitatively rules the thermal expansion. Generally, the thermal stability of the composite is quite good without any indication of possible disintegration.

The thermal expansion curves with corresponding coefficients of thermal expansion for CuCr1Zr/ZrB_2 composite are presented in Fig. 7. Both dependences are qualitatively and quantitatively quite similar to the Cu/ZrB_2 curves in Fig. 6. It indicates that the thermal expansion behaviour of pure Cu, as well as CuCr1Zr matrix, is comparable.

4. Discussion

Chemical analysis confirmed the composition of Cu, CuCr1Zr and ZrB_2 constituents. The binary B-Zr diagram in [13] shows that the ZrB_2 compound exists in a very narrow concentration range and there are no phase changes up to its melting point. The reason for the observed deviation in CTE in the temperature range 510 to 630 ℃ that was recorded for bulk ZrB_2 as well as for both composites must have some other reason. Obviously, it cannot be the result of some Cu-ZrB_2 or CuCr1Zr-ZrB_2 interaction as it appears already in bulk ZrB_2.

Paxton et al. [12] revealed that ZrB_2 with an anisotropic hexagonal structure exhibits directionally dependent properties. The coefficient of thermal expansion is different for *a*-axis and *c*-axis directions. They converge to the same value at around 780 K (507 ℃) below which CTE in *c*-axis is higher and above which CTE in *a*-axis is higher. As the observed deviation in CTE is in the vicinity of these temperatures, it is quite probable that it is to be related to this anisotropy in the thermal expansion of ZrB_2 itself.

Microscopy observations confirmed that for both composites good penetration of matrix metal had been achieved. In spite of poor wetting, the pores were filled with pressed metal during infiltration. The subsequent solidification and cooling caused the intimate contact between ceramics and metal matrix due to higher shrinkage of Cu and CuCr1Zr alloy. The observed pores were mostly located in the ZrB_2 preform. They belong to the population of closed pores that are not accessible to the molten matrix metal during infiltration.

Actually, no interfacial reaction took place for Cu neither for CuCr1Zr matrix. The interfacial bonding can be therefore regarded as of non-reactive nature. However, the structural stability of the composite up to the temperature of 800 ℃ appears quite good.

Typical relative elongations, as well as CTE, are compared in Fig. 8. It is clear that the lowest thermal expansion exhibits the ZrB_2 followed by the composites and both matrix metals.

The differences between Cu/ZrB_2 and CuCr1Zr/ZrB_2 composites are negligible. However, closer inspection of the thermal expansions in Fig. 9 reveals that maximum elongations recorded for particular heating/cooling cycles slightly increase for Cu/ZrB_2 composite and slightly decrease for CuCr1Zr/ZrB_2 composite (Fig. 9b). This indicates that the stability of the composite with CuCr1Zr matrix somewhat improves when subjected to the applied thermal cycling.

5. Conclusions

Cu/ZrB_2 and CuCr1Zr/ZrB_2 composites were suc-

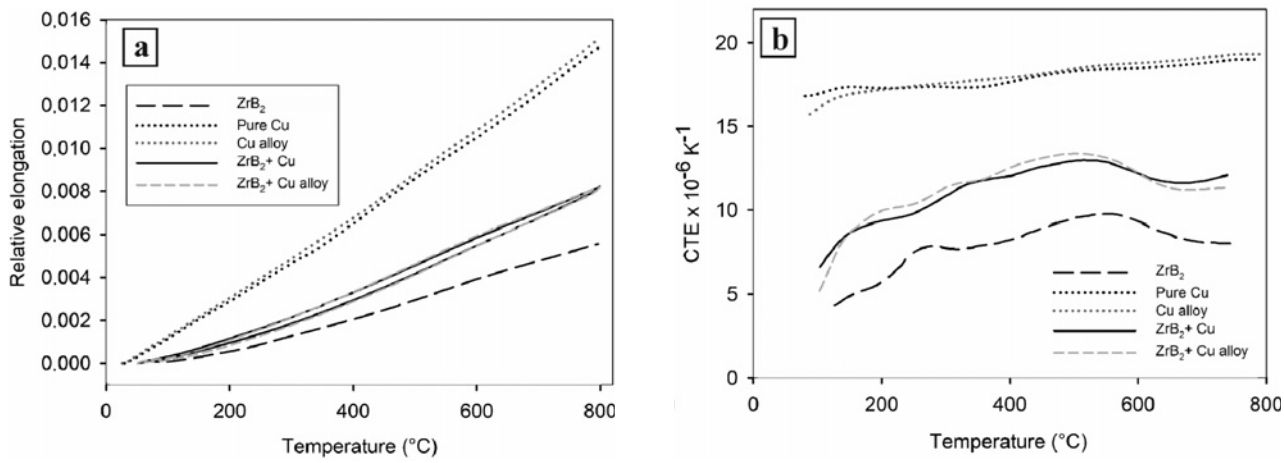

Fig. 8. Temperature dependences of relative elongations (a) and CTE (b) for ZrB_2, Cu/ZrB_2, CuCr1Zr/ZrB_2, Cu and CuCr1Zr recorded in the 5th cycle.

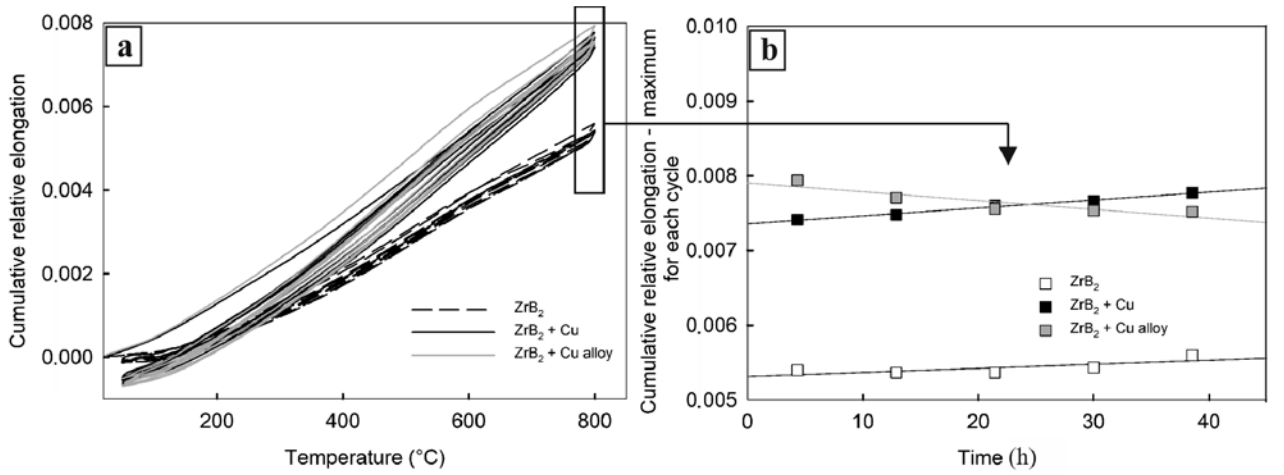

Fig. 9. Temperature dependencies of thermal expansion (a) and maximum elongations recorded for particular cycles (b).

cessfully prepared by gas pressure infiltration of ZrB_2 porous preform.

Pores observed in the structure of composites were identified as closed pores not accessible to the molten matrix metal during infiltration.

No substantial differences in the behaviour of composites were observed due to the matrix compositions.

No interfacial reaction was observed indicating that the bonding is of non-reactive nature.

Both composites exhibit high structural stability when subjected to 5 consecutive heating/cooling cycles to 800 ℃.

Acknowledgement

This work was supported by the Slovak Scientific Grant Agency (grant number VEGA 2/0172/16).

References

[1] Hong, Ch., Han, J., Zhang, X., Meng, S., Du, Sh.: J. Alloy Compd., *460*, 2008, p. 400. doi:10.1016/j.jallcom.2007.06.082

[2] Norasetthekul, S., Eubank, P. T., Bradley, W. L., Bozkurt, B., Stucker, B.: J. Mater. Sci., *34*, 1999, p. 1261. doi:10.1023/A:1004529527162

[3] Ju, J.-Y., Kim, Ch.-H., Kim, J.-J., Lee, J.-H., Lee, H.-S., Shin, Y.-D.: J. Elect. Eng. Tech., *4*, 2009, p. 538. doi:10.5370/JEET.2009.4.4.538

[4] Zimmermann, J. W., Hilmas, G. E., Fahrenholtz, W. G.: J. Am. Ceram. Soc., *91*, 2008, p. 1405. doi:10.1111/j.1551-2916.2008.02268.x

[5] Chamberlain, A. L., Fahrenholtz, W. G., Holmas, G. E.: J. Eur. Ceram. Soc., *29*, 2009, p. 3401. doi:10.1016/j.jeurceramsoc.2009.07.006

[6] Monteverde, F., Bellosi, A., Guicciardi, S.: J. Eur. Ceram. Soc., *22*, 2002, p. 279. doi:10.1016/S0955-2219(01)00284-9

[7] Zhu, S., Fahrenholtz, W. G., Hilmas, G. E., Zhang, S. C.: Mater. Sci. Eng. A, *459*, 2007, p. 167.

doi:10.1016/j.msea.2007.02.116
[8] Mallik, M., Kailath, A., Ray, K. K., Mitra, R.: J. Eur. Ceram. Soc., *32*, 2012, p. 2545. doi:10.1016/j.jeurceramsoc.2012.02.013
[9] Buyakova, S., Burlachenko, A., Mirovoi, Y., Sevostiyanova, I., Kulkov, S.: IOP Conf. Ser.: Mater. Sci. Eng., *140*, 2016, p. 012006. https://doi:10.1088/1757-899X/140/1/012006
[10] Muolo, M. L., Ferrera, E., Passerone, A.: J. Mater. Sci., *40*, 2005, p. 2295. doi:10.1007/s10853-005-1948-1
[11] Muolo, M. L., Ferrera, E., Novakovic, R., Passerone, A.: Scripta Mater., *48*, 2003, p. 191. doi:10.1016/S1359-6462(02)00361-5
[12] Paxton, W. A., Özdemir, T. E., Şavklıyıldız, İ., Whalen, T., Biçer, H., Akdoğan, E. K., Zhong, Zh., Tsakalakos, Th.: J. Ceram., *2016*, 2016, p. 8346563. doi:10.1155/2016/8346563
[13] Franke, P., Neuschütz, D.: In: Binary Systems. Part 5: Binary Systems Supplement 1. Landolt-Börnstein – Group IV Physical Chemistry (Numerical Data and Functional Relationships in Science and Technology). Berlin, Heidelberg Springer 2007. doi:10.1007/978-3-540-45280-5